Mausam, (1983), **34**, 1, 27-32

551.515.11

Behaviour of monsoon depressions in a primitive equation barotropic model

SURANJANA SAHA

School of Environmental Sciences, Jawaharlal Nehru University, New Delhi

(Received 29 December 1981)

सार – अरबसागर और बंगाल की खाड़ी पर से होकर जाने वाले मानसून अवदाबों का पूर्वानुमान लगाने के लिए एकल स्तरीय पूर्वंग समीकरण प्रतिदर्श को उपयोग में लाया गया है। इसमें उपयोग में लाए गए आंकड़े मानसून प्रयोग-1979(मानेक्स-79) के आंकड़ें हैं। प्रतिदर्श का संरूप उथले पानी की समीकरणों पर आधारित है। इसमें समाकलन की अवधि में परिसर पर कुल उर्जा एवं संहति की अविनाशिता के लिए परिमिति अवकलनी स्कीम अभिकल्पित की गई है। प्रतिदर्श का प्रारंभिक आगम पवन क्षेत्र का व्यक्तिनिष्ठ विश्लेषण है जिसमें संतुलित पवन संबंध का उपयोग करके भूविभव क्षेत्र व्युत्पन्न किया गया है। प्रतिदर्श समीकरणों के अविरोध संहति एवं पवन क्षेत्रों में संतुलन स्थापित करने के लिए गतिक प्रारंभीकरण को उपयोग में लाया गया है। तीन अवदाबों के गमन का अध्ययन किया गया है। यह प्रतिदर्श उनके गमन की शुद्धता का पूर्वानुमान एक निश्चित सीमा तक लगा सकता है। समाकलन की अवधि में कुल उर्जा अच्छी तरह से संरक्षित रहती है।

ABSTRACT. A single-level primitive equation model is used to predict the movement of monsoon depressions over the Arabian Sea and the Bay of Bengal. The data used are for the Monsoon Experiment-1979 (MONEX-79). The model formulation is based on shallow water equations. The finite-differencing scheme is designed to conserve total energy and mass over the domain during the course of integration. The initial input to the model is the subjectively analysed wind field from which geopotential field is derived through balance wind relation. Dynamic initialization is used to balance the mass and wind fields consistent with the model equations. The movement of three depressions has been studied. The model is able to predict their movement to a limited degree of accuracy. The total energy is conserved well during the course of integration.

1. Introduction

The quasi-geostrophic assumption has been found to be quite useful for predicting the behaviour of atmospheric flow in the middle and high latitudes. Over the tropical belts however, this assumption is not very satisfactory, particularly for regions close to the equator. Therefore, the quasi-geostrophic models are not very adequate for predicting the behaviour of the tropical atmosphere. A primitive equation model is comparatively better suited for this purpose. To predict the details of three dimensional flow, a multi-level primitive equation model incorporating friction, radiation processes, the hydrological cycle and air-sea interaction is necessary. However, verification statistics of models tried so far appear to suggest that for prediction of tropical systems, particularly tracks of circulation systems, a simple barotropic model often performs fairly well. Further, in the tropics, the pressure gradients are generally weak and often complicated by large observational errors. For this reason, the wind which is more accurate and numerous, is preferred to pressure or geopotential as basic input to tropical models. In the present paper, a simple single-level primitive equation barotropic model has been used with wind as input to predict the behaviour of monsoon depressions that formed in the Bay of Bengal and the Arabian Sea during the period of the Summer Monsoon Experiment (MONEX-1979).

2. Model equations

Shallow water equations in the flux form, neglecting friction, used in the formulation of the one-level primitive equation model are outlined below :

(*Symbols* used are described in Table 1)

$$\frac{\partial hu}{\partial t} = -D_2(u) + fhv - h\frac{\partial h}{a\cos\theta\,\partial\lambda} \qquad (1)$$

$$\frac{\partial hv}{\partial t} = -D_2(v) - fhu - h\frac{\partial h}{a\,\partial\theta} \qquad (2)$$

$$\frac{\partial h}{\partial t} = -D_2(1) \qquad (3)$$

where, $D_2(\ )$ is the horizontal flux divergence operator,

$$= \left\{ \frac{1}{a\cos\theta} \left(\frac{\partial h u(\ )}{\partial \lambda} + \frac{\partial h v(\ )\cos\theta}{\partial \theta} \right) \right\}$$

In this model, we assume a single layer of the atmosphere resting on the rigid surface of the earth, where the free surface is subject to variations in height depending on the nature of the flow. The free surface height in the present study corresponds to the height of the 500 mb surface at which the circulation patterns are considered.

3. Computational procedure

The finite difference formulation of the primitive equations listed above was designed, following Arakawa (1966) and Lilly (1965), to conserve momentum and kinetic energy over the computational domain. The horizontal flux divergence operator $D_2(\ )$, appearing in the model Eqns. (1) to (3), may be written in the finite difference form as :

$$D_2(\ ) = \frac{1}{a\cos\theta} \left\{ \frac{\delta_\lambda \overset{-\lambda}{(hu.(\ ))}}{\triangle\lambda} + \frac{\delta_\theta \overset{-\theta}{(hv.(\ ))}\cos\theta}{\triangle\theta} \right\}$$

where,

$$\delta_\lambda x = x\left(\lambda + \frac{\triangle\lambda}{2}\right) - x\left(\lambda - \frac{\triangle\lambda}{2}\right)$$

$$\delta_\theta x = x\left(\theta + \frac{\triangle\theta}{2}\right) - x\left(\theta - \frac{\triangle\theta}{2}\right)$$

and

$$\overset{-\lambda}{x} = \tfrac{1}{2}\left\{ x\left(\lambda + \frac{\triangle\lambda}{2}\right) + x\left(\lambda - \frac{\triangle\lambda}{2}\right) \right\}$$

$$\overset{-\theta}{x} = \tfrac{1}{2}\left\{ x\left(\theta + \frac{\triangle\theta}{2}\right) + x\left(\theta - \frac{\triangle\theta}{2}\right) \right\}$$

The height gradient terms in the finite difference form are :

$$\frac{\partial h}{a\cos\theta\,\partial\lambda} = \frac{\delta_\lambda \overset{-\lambda}{h}}{a\cos\theta\,\triangle\lambda}$$

$$\frac{\partial h}{a\,\partial\theta} = \frac{\delta_\theta \overset{-\theta}{h}}{a\,\triangle\theta}$$

$$\triangle\theta = \triangle\lambda = 2.5 \text{ degree}$$

4. Initial input

The basic input to the model consists of manually analysed streamline-isotach fields at 500 mb. The geopotential height field is obtained by solving the non-linear balance equation:

$$\nabla^2 h = \nabla\cdot\left(f\nabla\psi\right) + 2J\left(\frac{\partial\psi}{\partial x}, \frac{\partial\psi}{\partial y}\right) + \beta\frac{\partial\psi}{\partial y} \qquad (4)$$

The boundary conditions are the observed values of geopotential heights at the boundaries of the domain. Saha and Suryanarayana (1971) found that this type of balance relation described mutually consistent flow patterns in wind and geopotential fields in the tropics. To start with, the vorticity field is obtained from the observed wind field using the relation:

$$\zeta = \nabla^2\psi = \left\{ \frac{1}{a\cos\theta}\left(\frac{\partial v}{\partial\lambda} - \frac{\partial u\cos\theta}{\partial\theta}\right) \right\} \qquad (5)$$

Taking $\psi = 0$ at the lateral boundaries, the Poisson-type equation $\nabla^2\psi = \zeta$ is solved by Liebmann's successive relaxation scheme to obtain ψ — field. An over relaxation factor of 1.4 was found to be appropriate for quick convergence of the relaxation process. Five-point Jacobian and Laplacian operators are used to calculate the right hand terms of Eqn. (4) from the stream function values computed from Eqn. (5). Eqn. (4) is then solved using Liebmann's relaxation procedure to obtain a balanced geopotential field.

5. Dynamic initialisation and boundary conditions

The geopotential height field obtained in Section 4, through the non-linear balance equation, is in a static balance with the non-divergent part of the wind. The geopotential height patterns so arrived at, are thus, rather smoother than the actual observed patterns. In the tropics, the non-divergent part of the wind may be significant and hence, should be incorporated when arriving at a balance between the mass and velocity fields at the initial stages of integration of the model. This is achieved by a process of dynamic initialisation. For this, the model, with the observed wind and geopotential field as obtained in section 4, was integrated forward for one hour, followed by backward integration for one hour. Euler forward backward time integration scheme (Matsuno 1966) with a time step of six minutes was used during initialisation. The time integration scheme consists of two steps :

$$X^* = X(T) + \left(\frac{\partial X_T}{\partial t}\right)\cdot\triangle T$$

$$X(T+\triangle T) = X(T) + \left(\frac{\partial X^*}{\partial t}\right)\cdot\triangle T$$

where $X(T)$ and $X(T+\triangle T)$ are the values of variable X at time T and $T+\triangle T$, and X^* is its intermediate value.

Both the geopotential and wind fields are freely allowed to float during the initialisation process. No diffusive terms are taken into account during initialisation, as they represent irreversible processes. Initialisation extending upto 8 to 10 hours of model time was found to be sufficient to achieve a reasonable balance between wind and geopotential fields.

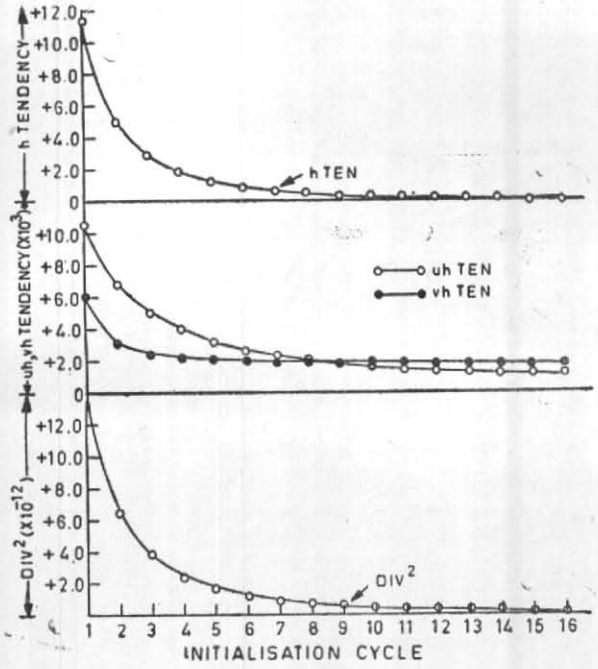

Fig. 1. Variation of height tendencies (*h* TEN), *uh* and tendencies (*uh* TEN, *vh* TEN) and divergence field (DIV) during dynamic initialisation

By this time, the height tendencies and divergence field got stabilised, as may be seen from Fig. 1.

Boundary conditions used were to ensure that no fluxes of momentum or mass were allowed across the domain boundaries. For this the east-west boundaries were closed by making them cyclic. This was done by introducing 7 extra grid points in the zonal direction (Krishnamurti 1968) on the eastern side, such that $A\ (1) = A\ (N+6)$ and $A(2) = A(N+7)$, where N is the number of grid points in the unextended mesh along the zonal direction and A's represent data values. With these boundary conditions, it is anticipated that as far as short range prediction of slow-moving meteorological systems are concerned, the errors are confined to the region outside forecast domain.

To ensure no flux across the northern and southern boundaries, meridional gradients of *v*, *uh*, *vh*, were made to vanish at these boundaries (Shuman and Vandermann, 1966).

6. Time integration

The model was integrated for a number of typical synoptic situations to produce 24-hour forecast fields. A centred time differencing scheme (leap-frog) with a time step of 6 minutes was used for this purpose. As initially the fields were available for only one time level, the first time step was the forward one.

The diffusive terms $\mu\nabla^2 u$ and $\mu\nabla^2 v$ were introduced in the equations for u and v tendencies (Eqns. 1 and 2). During the integration, with the diffusion constant $\mu = 1\times10^5$ m² sec^{-1}.

To avoid separation of solutions at alternate time steps arising out of computational mode of centred finite time differencing scheme, a mild Robert time filter (Robert 1966) is used during integration. This filter may be written as :

$$A^*_{t-1} = A_{t-1} + 0.05\,(A^*_{t-2} - 2A_{t-1} + A_t)$$

where A^* is the filtered value of A and the subscripts t, t—1, t—2 indicate time levels.

Except for the above filter, no other smoothening process was adopted during the course of integration. The 24-hour forecast output was found to contain some spurious two-grid wave noise which was filtered out by designing a Gaussian filter to effectively eliminate such noise (Shapiro 1970). The filter consists of two scans:

Scan *i*: $\bar{Z}_j = Z_j + \frac{1}{4}(Z_{j-1} - 2Z_j + Z_{j+1})$

Scan *ii*: $\bar{\bar{Z}}_j = \bar{Z}_j - \frac{1}{4}(\bar{Z}_{j-1} - 2\bar{Z}_j + \bar{Z}_{j+1})$

where Z_j is the unsmoothed value, $\bar{Z}_j$ is the smoothed value after the first scan and $\bar{\bar{Z}}_j$ is the final value.

It can be shown that the frequency response of this filter is given by :

$$R = 1 - \sin^2\left(\frac{m\pi\,\triangle x}{L}\right)$$

Thus the filter removes the two-grid waves completely without adversely affecting the larger important meteorological waves. To examine the energy conserving properties of the model, area averages of the following elements were monitored : (*i*) kinetic energy, (KE), (*ii*) square of relative vorticity, (TV2), (*iii*) total energy, (TE), *i.e.*, the sum of kinetic and potential energy and (*iv*) the sum of geopotential height values (SHGT).

7. Model, domain, grid, and data used

The model was applied to an area extending from 5.0°N to 35.0°N latitudes and from 60.0°E to 100°E longitudes with a 2.5° latitude/longitude grid for computation of the horizontal parameters. Input to the model was the wind direction and speed at each grid point obtained from the manual analysis of streamline-isotach fields at 500 mb. For the boundary conditions, the actual observed height values were taken at the grid points that formed the boundaries of the domain. Using MONEX-79 data, the model was applied to three synoptic situations each having a monsoon depression in the field, centred at 12 GMT of date as follows :

Date	*Position of centre of depression*
17 June 1979	14.5°N 65.0°E
6 July 1979	17.5°N 88.0°E
13 August 1979	21.5°N 91.5°E

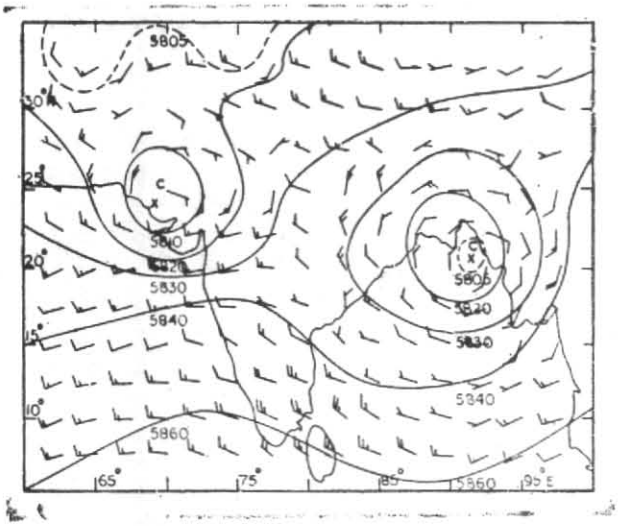

Fig. 2. Observed wind and height fields at 500 mb at 12 GMT, 13 August 1979 (solid lines indicate isobaric heights in metres)

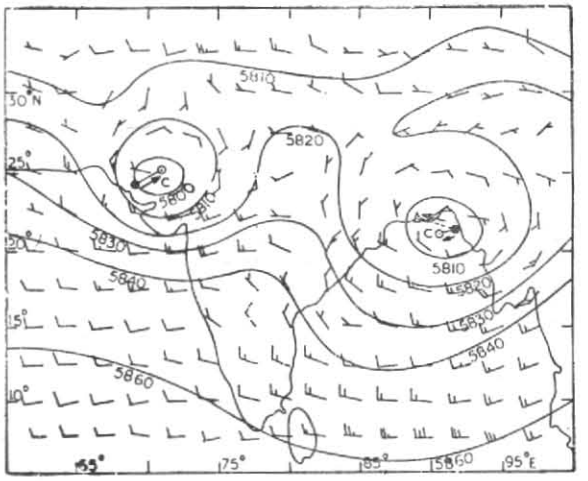

Fig. 4. Predicted 24-hour model forecast at 500 mb valid for 12 GMT, 14 August 1979

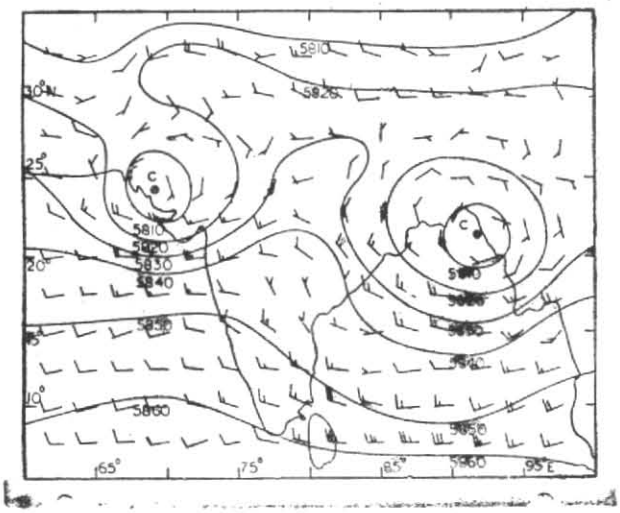

Fig. 3. Dynamically initialised wind and height fields at 500 mb at 12 GMT, 13 August 1979

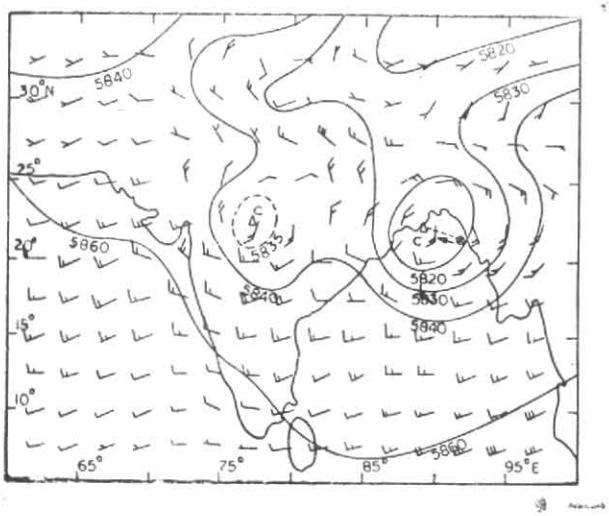

Fig. 5. Observed wind and height fields at 500 mb at 12 GMT, 14 August 1979

8. Results

Predicted wind and stream function patterns are compared to the non-divergent wind and stream function fields of the following day. Although the integrations were performed for all the situations mentioned in section 7, we present here the results of one situation only, for lack of space. Figs. 2, 3, 4, and 5 show the results of forecast in the case of the synoptic situation at initial maptime 12 GMT, 13 August 1979. As seen from Fig. 2, the centre of depression over the Bay of Bengal lies at 21.0°N 91.5°E. Another low pressure area lies over the western part of the country centred at 24.0°N 69.0°E. From Fig. 3, which represents the field after 16 hours of dynamic initialisation process, the Bay depression seems to have slightly shifted to the north and is now centred at 21.5°N 91.5°E. The other low has remained nearly stationary over the western part of the country and intensified to a very small extent. From the forecast field in Fig. 4, it may be seen that the Bay depression has moved to 21.5°N 90.5°E., while the other low has further intensified and now lies at 25.0°N 71.0°E. Finally, from Fig. 5, which gives the observed field at 12 GMT of 14 August 1979, the actual position of the depression over the Bay of Bengal is at 22.5°N 89.0°E, which indicates a faster movement of depression in a more northerly direction than the forecast movement

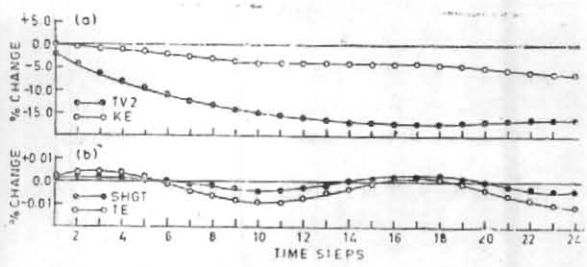

Fig. 6. Percentage change with time step in the area-averaged values of : (a) kinetic energy (KE) and square of relative vorticity (TV2) — the upper part; and (b) total energy (TE) and the sum of the geopotential height (SHGT)-the lower part

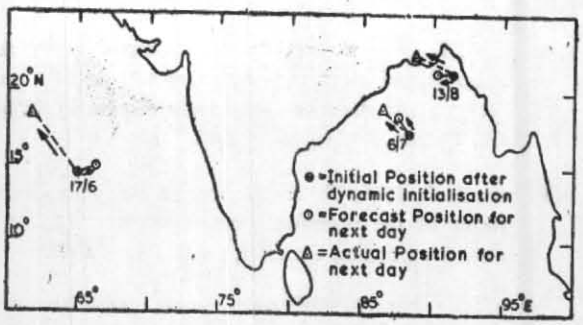

Fig. 7. Comparison of 24-hour forecast with observed position of the centre of depression for the three synoptic situations studied. Date/month of the depression are indicated near its initial position

The depression has also weakened to some extent. The low over the western part of the country has also weakened considerably.

The variation of the average values of kinetic energy, square of relative vorticity, total energy and sum of geopotential height as the percentage of their initial values, during the course of integration, are shown in Fig. 6 (a) and 6 (b). We notice that there is a decrease of about 6% in the case of kinetic energy and of about 16% in the case of the square of relative vorticity values. A change of 6% in the kinetic energy is equivalent to a change in wind speed less than 3%.

An examination of u and v variations separately shows that large part of this change is contributed by a change in the zonal kinetic energy. Relatively large changes in the vorticity values though not well understood may be partly due to the boundary conditions which do not strictly conserve vorticity and kinetic energy. From Fig. 6 (b) the variation in the total energy and the sum of the geopotential height values, follow each other closely in a sinusoidal pattern, but vary very negligibly above and below their initial values; the maximum increase for total energy is 0.005% and for SHGT is 0.003% while the maximum decrease for TE is 0.005% and for SHGT is 0.011%.

Fig. 7 gives the comparative performance of the model for the three synoptic situations studied. The depression in the central Arabian Sea on 17 June 1979 shows an unrealistic forecast movement, as compared to its actual movement. The prediction for the Bay of Bengal depression of 6 July 1979 was however quite good. It may be noted that except for the depression of 17 June 1979, the prediction of the westward component of the movement of the depressions agrees well with their actual movement. Errors lie mainly in predicting their meridional movements.

9. Conclusions

The study has shown that a single-level primitive equation barotropic model is able to predict the movement of monsoon depressions to a limited degree of accuracy. Inaccuracies in the prediction of movement of depressions or cyclones in the Indian region may arise out of several factors. Firstly, from the incorrectness of the analysis of the initial and verification wind fields, caused principally by lack of data. This is so, because depressions and cyclones generally form over the open seas, where conventional meteorological data especially upper wind data, are conspicuously lacking. Therefore, the initially observed charts may have large errors. Another important source of error lies in the large grid spacing. It is possible that reduction of grid length may lead to an improvement in the forecast accuracy and this requires closer examination. Also, a barotropic model cannot possibly give a good representation of conditions in a highly baroclinic atmosphere, such as the monsoon depression field, where diabatic heating due to the release of latent heat of condensation is very important.

Acknowledgements

Thanks are due to Dr. G. P. Malik, School of Environmental Sciences, Jawaharlal Nehru University, for his encouragement throughout this study and to Dr. P. K. Das, Director General of Meteorology, India Meteorological Department, for making available important MONEX-79 data on which this research work is based. The author also acknowledges the guidance and useful suggestions provided by Dr. K. R. Saha and Dr. H. S. Bedi during the course of this work. Mr. Saini carefully prepared all the diagrams and Mr. G. Hegde types the manuscript.

TABLE 1

List of symbols

θ	:	latitude
λ	:	longitude
h	:	height in metres
$\triangle\theta$	:	grid distance in north-south (Y) direction; 2.5 degree latitude
$\triangle\lambda$	:	grid distance in east-west (X) direction; 2.5 degree longitude
a	:	radius of the earth, 6371.229 km.
$\triangle x$	:	grid distance in $X-$direction in metres $= a \cos\theta \triangle\lambda$
$\triangle y$	:	grid distance in $Y-$direction in metres $= a\ \triangle\theta$
$\triangle t$	:	time interval, 6 minutes
g	:	acceleration due to gravity, 9.8 metres/sec^2
ϕ	:	geopotential height, gz
$\mathbf{V}$	:	horizontal wind vector
u, v	:	components of $\mathbf{V}$ in the $X-$ and $Y-$ directions respectively
Ω	:	angular velocity of the earth, 7.29×10^{-5}/sec
f	:	Coriolis parameter, $2\Omega \sin\theta$
β	:	$\frac{\partial f}{\partial y}$, $\frac{2\Omega\cos\theta}{a}$
ψ	:	stream function, defined by $\mathbf{V}=\mathbf{k}\times\nabla\psi$ where $\mathbf{k}$ is the vertical unit vector and ∇ is the horizontal Nabla operator
ζ	:	relative voritcity, $\nabla^2\psi$
∇^2	:	Laplacian operator $=\left(\frac{\partial^2}{\partial x^2}+\frac{\partial^2}{\partial y^2}\right)$
$J(a,b)$	:	Jacobian operator $\left(\frac{\partial a}{\partial x}\frac{\partial b}{\partial y}-\frac{\partial a}{\partial y}\frac{\partial b}{\partial x}\right)$

References

Arakawa, A., 1966, Computational design for long term numerical integrations of the equations of atmospheric motion, *J. Computational Physics*, **1**, 119-143.

Krishnamurti, T.N., 1969, An experiment in numerical prediction in the equatorial latitudes : *Quart. J. R. Met. Soc.*, **95**, pp. 594-620.

Lilly, D. K., 1965, On the computational stability of numerical solutions of time-dependent, nonlinear geophysical Fluid Dynamics problems, *Mon. Weath. Rev.*, **93**, 1, pp. 11-26.

Matsuno, T, 1966, A finite difference scheme for the time integration of oscillatory equations with second order accuracy and sharp cutoff for high frequencies, *J. met. Soc.*, Japan, **44** (1), pp. 85-88.

Robert, A. J., 1966, The integrations of low order spectral forms of the primitive meteorological equations, *J. met. Soc.*, Japan, Series II, **44**, 5, pp. 237-245.

Saha, K. R. and Suryanarayana, R., 1971, Numerical solutions of geopotential with different forms of balance relationships in the tropics, *J. met. Soc.*, Japan, Series II, **49**, pp. 510-515.

Shuman F. G. and Vandermann, L. W., 1966, Difference system and boundary conditions for the primitive equation barotropic forecast, *Mon. Weath. Rev.*, **94**. pp. 329-335.

Shapiro, R., 1970, Smoothing, filtering and boundary effects, *Rev. Geophys. and Space Phys.*, **8**, pp. 359-387.